



# Electric field-assisted sintering (gadolinia-doped ceria/alkali salts) composite membranes

S.G.M. Carvalho<sup>a,\*</sup>, E.N.S. Muccillo<sup>a</sup>, F.M.B. Marques<sup>b</sup>, R. Muccillo<sup>a</sup>

<sup>a</sup> Center of Science and Technology of Materials – CCTM, Energy and Nuclear Research Institute – IPEN, S. Paulo, SP 05508-000, Brazil

<sup>b</sup> Department of Materials Engineering and Ceramics, University of Aveiro, Portugal

## ARTICLE INFO

### Keywords:

Composite electrolytes

Flash sintering

Impedance spectroscopy

## ABSTRACT

Composite ceramic membranes were prepared according to two routes: (i) vacuum impregnation of molten eutectic sodium-lithium carbonates (NLC) into porous ceria-20 mol% gadolinia (20GDC) solid electrolytes; (ii) electric field-assisted sintering of a 25 wt% NLC/75 wt% 20GDC mixture. Porous 20GDC ceramics were obtained by controlled thermal removal of 40 vol% KCl added as pore former. Electric field-assisted (flash) sintering was carried out monitoring thickness during application of 200 V cm<sup>-1</sup> to the specimen positioned in a sample chamber inserted in a vertical dilatometer. The surfaces of the sintered membranes were observed in a scanning electron microscope. Electrochemical impedance spectroscopy measurements were performed in the 5 Hz to 13 MHz frequency range in the 280–580°C range. Arrhenius plots showed the transition from oxide ion conduction (due to the solid electrolyte) to carbonate ion conduction (due to the molten NLC). Membranes flash sintered at 420°C in 2 min showed electrical conductivity similar to membranes conventionally sintered at 690°C for 2 h.

## 1. Introduction

Ceramic membranes find a wide range of application in devices for gas separation, particularly for carbon dioxide, which is considered a main responsible for the greenhouse effect [1–3]. Among several approaches to efficiently separate carbon dioxide, a promising one operating at high temperature is the composite dual-phase membrane consisting of an oxide ion conducting matrix with a eutectic mixture, i.e. a mixture such that all components melt simultaneously, without separation, of carbonate ion conducting alkali carbonates [4–8]. Several extensive reports were published on the properties of those membranes, showing methods for preparation, microstructural analysis, electrochemical properties, permeation rates, etc. [9–11].

Processing of composite membranes is not trivial. After conformation, sintering is the step required to produce the membrane with microstructure and mechanical strength adequate for handling and operating at temperatures higher than the carbonates eutectic temperature. However, there is a problem in sintering a composite ceramic membrane with large difference between their conventional sintering temperature.

Low temperatures would not be appropriate to sinter the matrix and high temperatures would promote evaporation of the carbonates. This problem is circumvented by producing a porous matrix and impregnating it with molten carbonates [6].

Since 2010 a new pressureless sintering technique is intensively explored to obtain dense ceramics by applying an electric voltage at temperatures and times lower than those used in conventional sintering in green pellets, named flash sintering. The time elapsed while the specimen shrinks ranges from seconds to a few minutes [12]. This technique requires an electric current limited power supply, connected via platinum leads to a sample inserted in a furnace [13]. Even though detailed mechanisms responsible for that sintering technique are still under debate, Joule heating promoted by the electric current is unambiguously the primary contribution to neck formation among particles and densification [14–18].

In this work we report for the first time the preparation of electric-field assisted pressureless sintering of composite dual-phase membranes of gadolinia-doped ceria and lithium-sodium carbonates. A comparison with samples conventionally sintered is also presented.

\* Corresponding author.

E-mail addresses: [sabrina.carvalho@usp.br](mailto:sabrina.carvalho@usp.br) (S.G.M. Carvalho), [enavarro@usp.br](mailto:enavarro@usp.br) (E.N.S. Muccillo), [fmarques@ua.pt](mailto:fmarques@ua.pt) (F.M.B. Marques), [muccillo@usp.br](mailto:muccillo@usp.br) (R. Muccillo).

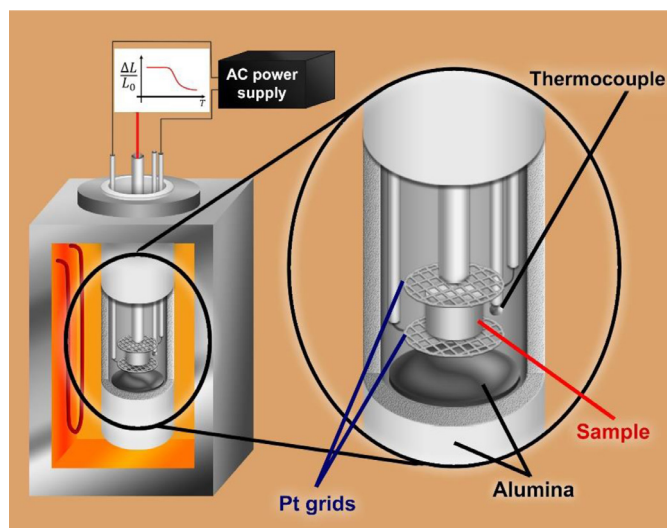


Fig. 1. Schematic view of the dilatometer furnace with the sample positioned between platinum electrodes for flash sintering experiments.

## 2. Experimental

CeO<sub>2</sub>: 20 mol% Gd<sub>2</sub>O<sub>3</sub> (> 100 m<sup>2</sup> g<sup>-1</sup> specific surface area, 20GDC, Fuel Cell Materials, USA), sodium and lithium carbonates mixed to 52 mol%:48 mol% Na<sub>2</sub>CO<sub>3</sub>:Li<sub>2</sub>CO<sub>3</sub> (NLC, Alfa Aesar, 99%) and KCl (Alfa Aesar, 99%) were used as precursors. Composite ceramic membranes were prepared following two different routes:

- (1) Impregnating porous 20GDC with NLC.

To prepare porous 20GDC, 40 vol% KCl was added and the composition was ball milled with zirconia grinding media (Tosoh, Japan) for 2 h in ethanol; afterwards, the mixture was uniaxially (50 MPa) and isostatically (200 MPa) pressed to 14 mm diameter pellets, heated at 1°C min<sup>-1</sup> up to 800°C for 3 h for thermal removal of KCl, followed by heating to 1450°C for 1 h, and cooling to room temperature at 1°C min<sup>-1</sup>. The apparent density of the sintered pellets was determined by the Archimedes technique.

For impregnation with NLC, the 20GDC sample was positioned on one end of an L-shaped quartz tube covered by NLC powder. The quartz tube was inserted in a resistive furnace and heated to 550°C (higher than the NLC melting point, 501°C). At that temperature the other side of the tube is connected to a vacuum pump to improve impregnation of the molten carbonates into the pores of the matrix. The sample surfaces were cleaned ultrasonically in distilled water.

- (2) Electric field-assisted sintering of a mixture of 20GDC with NLC.

A mixture of 75 wt% of 20GDC and 25 wt% of NLC (49:51 vol%) obtained by ball milling for 2 h in ethanol was uniaxially and isostatically pressed into a 5 mm diameter cylindrical shape and sintered at 420°C by applying 200 V cm<sup>-1</sup> AC electric field, 1 kHz, limiting the electrical current to 1 A. For the electric field-assisted (flash) sintering experiments, the ceramic green pellet was positioned between two platinum electrodes connected to a commercial power supply (Pacific Power Source 118-ACX, Irvine, CA, USA) with 20 A and 100 V as current and voltage limits, respectively, and inserted in the sample holder of a vertical dilatometer (model 1161, Anter, USA) as shown in Fig. 1.

Some samples were also sintered at different temperatures in a resistive furnace for further comparison of shrinkage levels with and without the application of an electric field.

Scanning electron microscopy (Inspect F50 FEG-SEM, FEI, Brno, Czech Republic) was used to observe surfaces of sintered and impregnated samples.

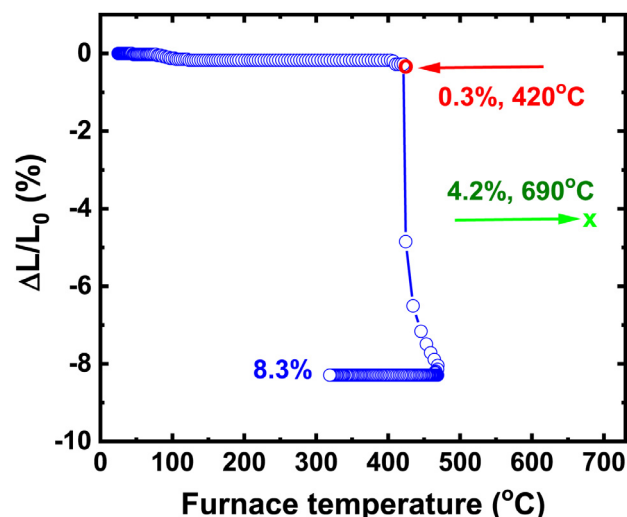


Fig. 2. Dilatometric curves of 20GDC + 25 wt% NLC for samples sintered at 420°C (●); sintered at 690°C for 2 h: (x); and sintered with an applied electric field (200 V cm<sup>-1</sup>, 1 kHz, at 420°C for 2 min, limiting electric current 1 A) at 420°C (○).

The electrical behavior of all samples was analyzed by impedance spectroscopy. Measurements were carried out in the 250–580 °C range with a Solartron SI 1260 Impedance/Gain-phase Analyzer in the 1 Hz to 10 MHz frequency range with 200 mV signal amplitude. The specimens had the parallel surfaces covered with silver paste with the organic binder thermally removed at 250°C. Afterwards they were positioned inside an Inconel 600 sample chamber with platinum leads and a chromel-alumel thermocouple located close to the sample. The entire cell was inserted in a programmable resistive furnace.

## 3. Results and discussion

Fig. 2 shows the linear thickness shrinkage of a 20GDC + 25 wt% NLC pellet upon heating from room temperature to 420°C. After reaching 420°C, an electric field was applied, as described in the experimental section. In the same figure, the reductions of the thickness of a similar sample heated to 420°C without applying the electric field and of another sample sintered at 690°C for 2 h, are also depicted.

The application of the AC electric field for 2 min at 420°C promoted 8.3% thickness shrinkage. The explanation is that the sample reached temperatures higher than 400°C due to the Joule heating produced by the electric current through the sample. Those temperatures were sufficient to melt the eutectic mixture of the carbonates, facilitating the percolation of an electric current, leading to an abrupt decrease of the electrical resistivity of the composite membrane. Electric field assisted sintering at higher temperatures could produce denser membranes, but Joule heating would be large enough to remove the carbonates by combined decomposition, vaporization and capillarity effects. Without applying the electric field at 420°C, the sample thickness shrank only 0.3%. Sintering at 690°C for 2 h [19], that value was 4.2%, approximately half the value attained with electric field-assisted sintered samples.

Fig. 3 shows the electric field and current versus time profiles collected during the electric field-assisted sintering experiment. There was a short time delay for the occurrence of a voltage spike due to the decrease of the electric resistivity produced by the increase of the temperature (Joule heating). The electric field decreased afterwards to maintain constant the pre-set electric current value.

For the membranes prepared by impregnation with molten carbonates, the ceramic porous matrix was first prepared by adding an alkali halide as sacrificial pore former, as described. Fig. 4 shows SEM images obtained at the surface of these samples. The addition of KCl promoted

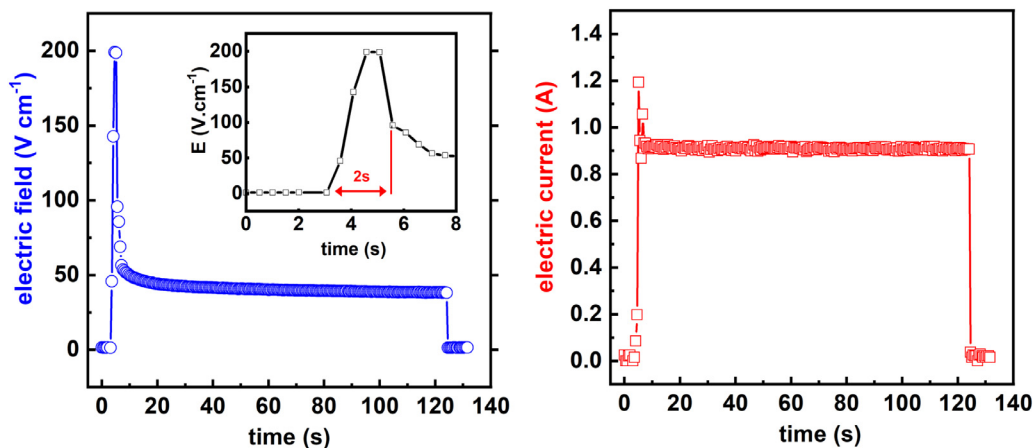


Fig. 3. Electric field and current during electric field-assisted sintering of 20GDC + 25 wt% NLC. Inset: exploded view of the first 8 s.

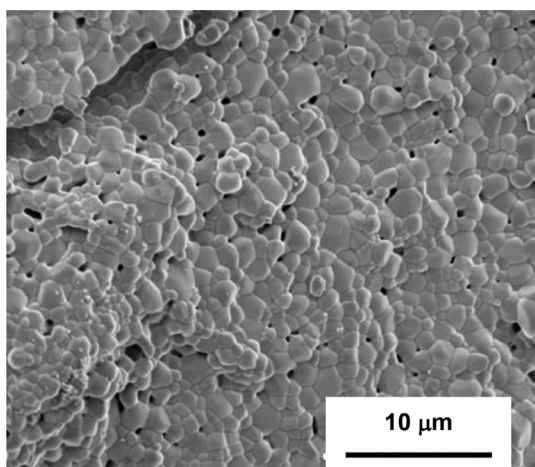


Fig. 4. FEG-SEM image of the surface of a porous 20GDC skeleton.

macro and micrometer pore sizes in the sintered sample. Impregnation depends on the wettability of the oxide phase and the viscosity of the

molten phase. Larger and open pores are easily filled during impregnation with lithium-sodium carbonates. Smaller and isolated pores are not so easily impregnated. The ceramic grains show a narrow average grain size, in the 1–2 μm range.

Fig. 5 shows typical FEG-SEM images of the sample surface after impregnation showing that the sodium-lithium carbonates composition was apparently not evenly distributed. These figures show a region fully covered with the carbonate (5a) and another with visible neck formation of grains on the 20GDC ceramic surface poorly covered with carbonate (5b).

Fig. 6 shows typical SEM images collected at the outer parallel surfaces (6a and 6c) and internal (fracture) surfaces of the electric field-assisted sintered sample. Fig. 6(a) and (b) are micrographs taken at the ceramic pellet surfaces while Fig. 6(c) and (d) were obtained after ultrasonically cleaning the ceramic pellets for removal of the carbonate phase.

At different regions of the samples sintered by applying an electric field at 420°C, both carbonate and 20GDC ceramic phases are observed. Unlike the samples impregnated with molten carbonate, which looked like cooled molten salt, the eutectic mixture of carbonates in the flash sintered samples consists of bars/fibers, produced by instantaneous

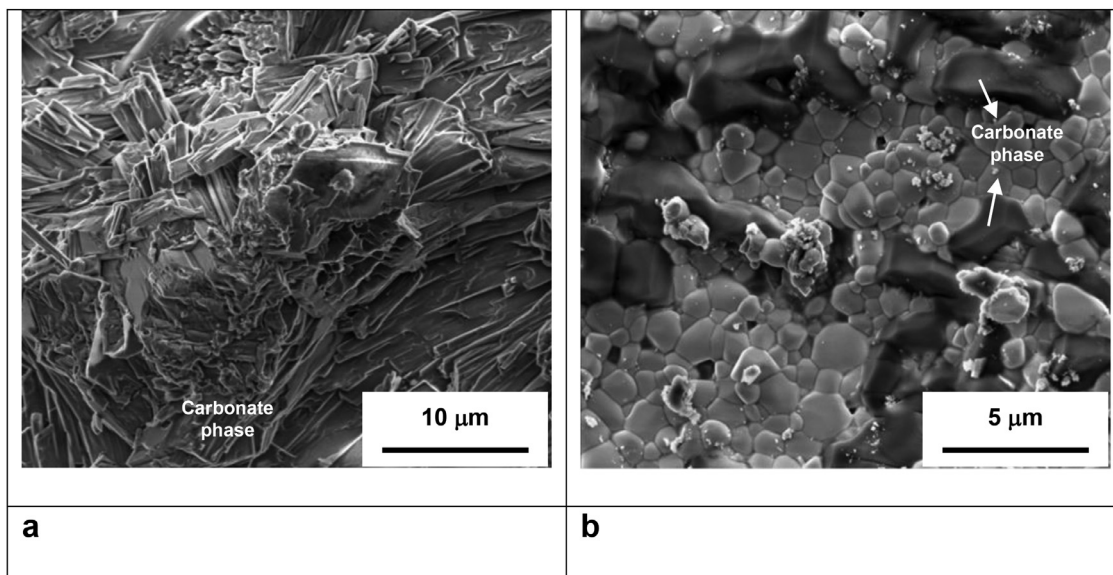
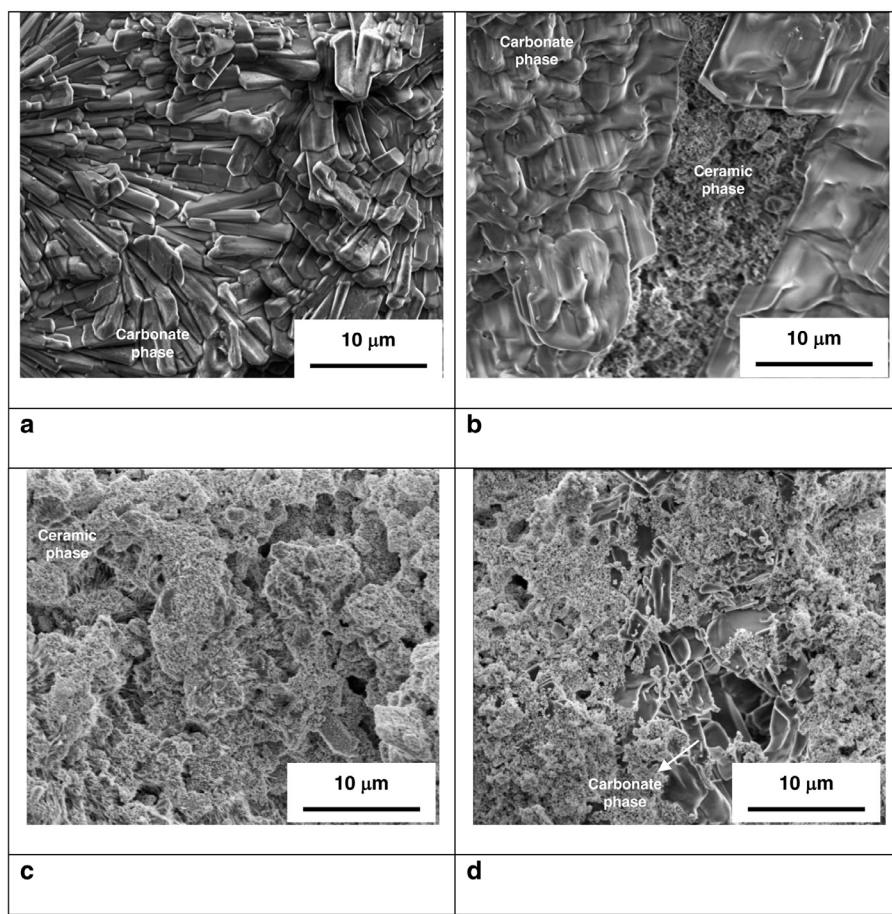
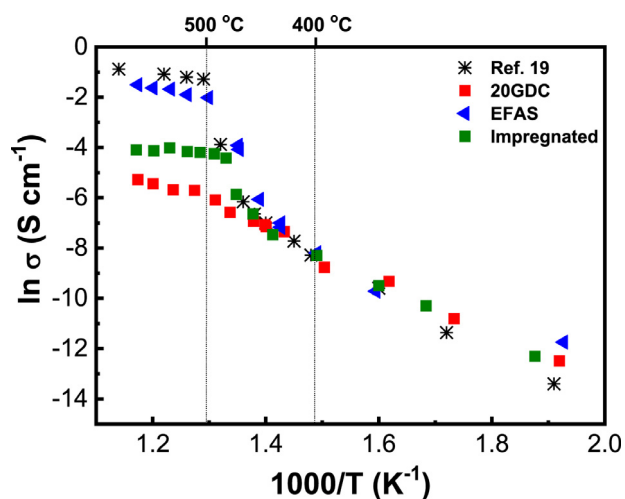


Fig. 5. SEM images of surfaces of porous 20GDC at two regions (a) and (b) of the sample surface after impregnation with molten sodium-lithium carbonates.



**Fig. 6.** SEM images of 20GDC + 25 wt% NLC sintered at 420°C with application of 200 V cm<sup>-1</sup>, 1000 Hz, 1 A electric current limit. (a) Outer surface; (b) fracture surface, (c) and (d) are images of the same samples after ultrasonically cleaning.



**Fig. 7.** Arrhenius plots of the electrical conductivity of the composite 20GDC with molten carbonates produced by impregnation of porous 20GDC matrix and by electric field-assisted sintering (EFAS). Also shown data of a dense 20GDC and from Ref. [19].

melting due to Joule heat promoted by the sudden flow of the electric current.

Fig. 7 shows Arrhenius plots of the electrical conductivity of the composite membranes produced by electric field-assisted sintering, by impregnation with molten carbonates, and of a pure (without pore former) 20GDC dense sample sintered according to the same temperature profile used to produce porous matrices. Data taken for 20GDC+NLC sintered

conventionally at 690°C for 1 h is also plotted for comparison purposes [19].

The Arrhenius plot of the electrical conductivity of the dense 20GDC sample exhibits mostly a linear behavior in the logarithmic scale for the entire temperature range, with an activation energy of 0.87 eV, showing that the electrical conductivity of the sample is dominated by conduction only by oxide ions through the oxide. The ceramic pellets containing carbonates have dominant mechanisms depending on the temperature range. At temperatures below 400°C the electrical conductivity of the membrane is basically due to oxide ion conduction via the 20GDC ceramic phase with an activation energy of 0.91 eV, in agreement with published results (0.907 eV [20], 0.90 eV [21], 0.88–0.99 eV [22]). From approximately 400–500°C the electrical conductivity increases steeply due to the contribution of the molten alkaline carbonates, enhancing charge transport. Between temperatures around 400°C and higher than 500°C, the conductivity increases up to four orders of magnitude. In the upper temperature range the conductivity follows again an Arrhenius behavior, situation ascribed to carbonate and alkali ions using molten salt pathways, with an activation energy of 0.32 eV, in good agreement with reported values for the eutectic mixture of potassium, lithium and sodium carbonates (0.326 eV [23]).

Carbon dioxide separation using composite membranes relies on the ambipolar transport corresponding to the net counter flow of oxide and carbonate ions in the distinct phases. Since at working temperatures the conductivity of the molten phase is much higher than the conductivity of the ceramic, ideal microstructures are those providing the best ceramic oxide percolation and minimum interfacial (grain boundary) resistance, as the oxide-ion transport is rate determining. Observation of lower temperature data, where the oxide phase has a superior ionic conductivity, provides a strong indication on the relative quality of ceramic skeletons

used in distinct membranes. In these conditions the electric field-assisted sintered sample shows a performance slightly higher than previously reported [19]. On the contrary, the relatively modest high temperature performance of the hereby impregnated sample with respect to literature data suggests a poor percolation of the NLC phase, probably due to the disparate pore sizes with poor connectivity, observed in Fig. 4. Overall, pressureless sintering at relatively low temperature with application of low voltages may be an alternative technique for preparing composite membranes with oxide ion conducting solid electrolytes and mixtures of alkali carbonates.

#### 4. Conclusions

Gadolinia-doped ceria/sodium-lithium carbonates (20GDC-NLC) composite membranes, proposed for carbon dioxide separation, were successfully sintered at 420°C under the application of a low AC electric field (200 V cm<sup>-1</sup>, 1 kHz). Their electrical conductivity was similar to reported values for membranes sintered at 690°C and higher than that of membranes obtained by impregnation of molten NLC into porous 20GDC matrices.

#### Funding

Financial support for this work was provided by Comissão Nacional de Energia Nuclear – CNEN, Fundação de Amparo à Pesquisa do Estado de São Paulo – FAPESP [CINE – Shell (ANP)/FAPESP 2017/11937-4 and CEPID-CDMF Proc. 2013/07296-2], and Conselho Nacional de Desenvolvimento Científico e Tecnológico – CNPq (Procs. 302357/2018-1, 305889/2018-4).

#### Declaration of Competing Interest

The authors declare that they have no known competing financial interests or personal relationships that could have appeared to influence the work reported in this paper.

#### Acknowledgment

S.G.M.C. holds a post-doctoral fellowship provided by Shell under CINE-Shell (ANP)/FAPESP Proc. 2017/11937-4.

#### References

- [1] O. Kaarstad, Fossil fuels and responses to global warming, *Energy Convers. Manag.* 36 (1995) 869–872, doi:10.1016/0196-8904(95)00141-Y.
- [2] S. Shafiee, E. Topal, When will fossil fuel reserves be diminished? *Energy Policy* 37 (2009) 181–189, doi:10.1016/j.enpol.2008.08.016.
- [3] S.S. Hashim, A.R. Mohamed, S. Bhatia, Oxygen separation from air using ceramic-based membrane technology for sustainable fuel production and power generation, *Renew. Sustain. Energy Rev.* 15 (2) (2011) 1284–1293, doi:10.1016/j.rser.2010.10.002.

- [4] B. Zhu, X.T. Yang, J. Xu, Z.G. Zhu, S.J. Ji, M.T. Sun, J.C. Sun, Innovative low temperature SOFCs and advanced materials, *J. Power Sources* 118 (2003) 47–53, doi:10.1016/S0378-7753(03)00060-0.
- [5] R. Raza, H. Qin, L. Fan, K.i Takeda, M. Mizuhata, B. Zhu, Electrochemical study on co-doped ceria-carbonate composite electrolyte, *J. Power Sources* 201 (2012) 121–127, doi:10.1016/j.jpowsour.2011.10.124.
- [6] S.G. Patricio, E. Papaioannou, G. Zhang, I.S. Metcalfe, F.M.B. Marques, High performance composite CO<sub>2</sub> separation membranes, *J. Membr. Sci.* 471 (2014) 211–218, doi:10.1016/j.memsci.2014.08.007.
- [7] A. Thursfield, I.S. Metcalfe, The use of dense mixed ionic and electronic conducting membranes for chemical production, *J. Mater. Chem.* 14 (2004) 2475–2485, doi:10.1039/b405676k.
- [8] J.J. Tong, L.L. Zhang, M.F. Han, K. Huang, Electrochemical separation of CO<sub>2</sub> from a simulated flue gas with high-temperature ceramic-carbonate membrane: New observations, *J. Membr. Sci.* 477 (2015) 1–6, doi:10.1016/j.memsci.2014.12.017.
- [9] Z.B. Yang, Y.M. Zhu, M.F. Han, Synthesis and characterization of gadolinium doped ceria-carbonate dual-phase membranes for carbon dioxide separation, *J. Alloys Compd.* 723 (2017) 70–74, doi:10.1016/j.jallcom.2017.06.164.
- [10] W. Zhu, C. Xia, D. Ding, X. Shi, G. Meng, Electrical properties of ceria-carbonate composite electrolytes, *Mater. Res. Bull.* 41 (2006) 2057–2064, doi:10.1016/j.materresbull.2006.04.001.
- [11] S.G. Patricio, E.I. Papaioannou, B.M. Ray, I.S. Metcalfe, F.M.B. Marques, Composite CO<sub>2</sub> separation membranes: insights on kinetics and stability, *J. Membr. Sci.* 541 (2017) 253–261, doi:10.1016/j.memsci.2017.07.008.
- [12] M. Cologna, B. Rashkova, R. Raj, Flash sintering of nanograin zirconia in < 5 s at 850°C, *J. Am. Ceram. Soc.* 93 (2010) 3556–3559, doi:10.1111/j.1551-2916.2010.04089.x.
- [13] R. Muccillo, E.N.S. Muccillo, An experimental setup for shrinkage evaluation during electric field-assisted flash sintering: application to yttria-stabilized zirconia, *J. Eur. Ceram. Soc.* 33 (2013) 515–520, doi:10.1016/j.jeurceramsoc.2012.09.020.
- [14] C.E.J. Dancer, Flash sintering of ceramic materials, *Res. Express* 3 (2016) 1–25, doi:10.1088/2053-1591/3/10/102001.
- [15] M. Yu, S. Grasso, R. Mckinnon, T. Saunders, M.J. Reece, Review of flash sintering: materials, mechanisms and modelling, *Adv. Appl. Ceram.* 116 (2017) 24–60, doi:10.1080/17436753.2016.1251051.
- [16] R. Muccillo, E.N.S. Muccillo, Electric field assisted sintering of electroceramics and in situ analysis by impedance spectroscopy, *J. Electroceram* 38 (2017) 34–42, doi:10.1007/s10832-016-0054-x.
- [17] O. Guillon, C. Elsässer, O. Gutfleisch, F. Janek, S. Korte-Kerzel, D. Raabe, C.A. Volkert, Manipulation of matter by electric and magnetic fields: Toward novel synthesis and processing routes of inorganic materials, *Mater. Today* 21 (2018) 527–536, doi:10.1016/j.mattod.2018.03.026.
- [18] M. Biesuz, V.M. Sglavo, Flash sintering of ceramics, *J. Eur. Ceram. Soc.* 39 (2019) 115–143, doi:10.1016/j.jeurceramsoc.2018.08.048.
- [19] M.I. Asghar, S. Jouttijärvi, R. Jokiranta, P.D. Lund, Remarkable ionic conductivity and catalytic activity in ceramic nanocomposite fuel cells, *Int. J. Hydrogen Energy* 43 (2018) 12892–12899, doi:10.1016/j.ijhydene.2018.05.045.
- [20] V. Esposito, E. Traversa, Design of electroceramics for solid oxide fuel cell application: playing with ceria, *J. Am. Ceram. Soc.* 91 (2008) 1037–1051, doi:10.1111/j.1551-2916.2008.02347.x.
- [21] R.M. Batista, A.M.D.C. Ferreira, E.N.S. Muccillo, Sintering and electrical conductivity of gadolinia-doped ceria, *Ionics* 22 (2016) 1159–1166, doi:10.1007/s11581-016-1648-7.
- [22] K. Neuhaus, R. Dolle, H.-D. Wiemhofer, Assessment of the effect of transition metal oxide addition on the conductivity of commercial Gd-doped ceria, *J. Electrochem. Soc.* 165 (2018) F533–F542, doi:10.1149/2.1111807jes.
- [23] E.V. Nikolaeva, I.D. Zakir'yanova, A.L. Bove, Electric conductivity of α-Al<sub>2</sub>O<sub>3</sub> suspensions in carbonate and carbonate-chloride melts, *Russian J. Electrochem.* 54 (2018) 690–696, doi:10.1134/S1023193518090094.